ELSEVIER

Biochimica et Biophysica Acta 1200 (1994) 161–166

BBA Biochimica et Biophysica Acta

Proton NMR study of the heme complex of hemopexin

Ruba S. Deeb [a,1], Ursula Muller-Eberhard [b], David H. Peyton [a,*]

[a] Department of Chemistry Portland State University, Portland, OR, 97207-0751, USA
[b] Department of Pediatrics, Pharmacology, and Biochemistry Cornell University Medical College, New York, NY 10021, USA

Received 10 September 1993

Abstract

Proton nuclear magnetic resonance spectroscopy of the complex of heme with hemopexin, a plasma protein with an exceptionally high affinity for heme, is reported. Characteristic spectra are shown for heme · hemopexin of cow, human, rabbit, and rat. Each of these spectra demonstrate that the iron of heme bound by hemopexin is paramagnetic and low-spin. Rabbit heme · hemopexin, which exhibits the best signal-to-noise ratio, is studied in detail. Deuterium isotope labeling experiments indicate that the methyls in heme positions 1-, 3-, and 8- are resolved downfield from the protein envelope of resonances; the 5-methyl may lie in the −5 to +12 ppm region. Two-dimensional nuclear Overhauser effect spectroscopy locates other protons of the heme periphery, including from the 2-vinyl. Strongly relaxed upfield resonances are identified and assigned to protons on the axial ligands. Cyanide interaction with heme · hemopexin produces an additional low-spin adduct.

Key words: Hemopexin; ^{1}H-NMR; Heme complex

1. Introduction

The interactions of the iron of heme with molecular oxygen causes the formation of oxygen radicals that damage lipids [1] and proteins [2,3]. Circulating heme-binding proteins may, therefore, be crucial to inactivate the potentially harmful heme occurring in states of hemolysis. The plasma protein hemopexin (Hx), present in substantial concentrations (~ 0.5–2 M) [4], has two outstanding properties: it inhibits heme-catalyzed oxidation reactions [5,6], and exhibits the highest affinity for heme [7]. Three other facts attest to a protective function of Hx against heme-catalyzed oxidations: (1) heme · Hx is cleared from the circulation selectively [8,9], (2) Hx is in most species an acute phase reactant [4], i.e., its synthesis is increased following oxidative stress [10] and injection of small amounts of heme [11,12], and (3) Hx extracts heme from erythrocyte membranes [13].

The physical reasons for the extremely tight interaction of Hx with heme are not well understood. A detailed structural analysis is not available, as Hx could not be crystallized, probably because of its extensive glycosylation, 20% by weight of a 60 kDa peptide chain [14,15]. In contrast to what might be expected, considering the strong inhibition of heme-catalyzed oxidations by Hx, the free exposure to solvent [16] suggests that heme is bound at the surface of Hx. The combined data on chemical modification [17,18] and proteolytic digestion [19], magnetic circular dichroism spectroscopy [20], and comparison of the sequences of two Hx species [10] indicate that two histidines ligate the heme iron. This is indicated in Fig. 1A; Fig. 1B shows the heme numbering system used. One of the axial ligands can be replaced, either by CO when heme · Hx is in the Fe^{II}-state [21], or by CN^- when heme · Hx is in the Fe^{III}-state [22].

^{1}H-NMR studies of heme proteins in their paramagnetic states have been applied in defining heme pocket structures and biological function [23]. The potential of probing

* Corresponding author. Fax: +1 (503) 7253888.

[1] Present address: Department of Biochemistry Cornell University Medical College, New York, New York 10021.

Abbreviations: DEAE, diethylaminoethyl; DSS, sodium 2,2-dimethyl-2-silapentane sulfonate; heme · Hx, the complex of heme with hemopexin; Hx, hemopexin; NOE, nuclear Overhauser effect; NOESY, two-dimensional nuclear Overhauser effect spectroscopy; NMR, nuclear magnetic resonance; SDS-PAGE, sodium dodecyl sulfate-polyacrylamide gel electrophoresis; TPPI, time-proportional phase incrementation

SSDI 0304-4165(94)00012-M

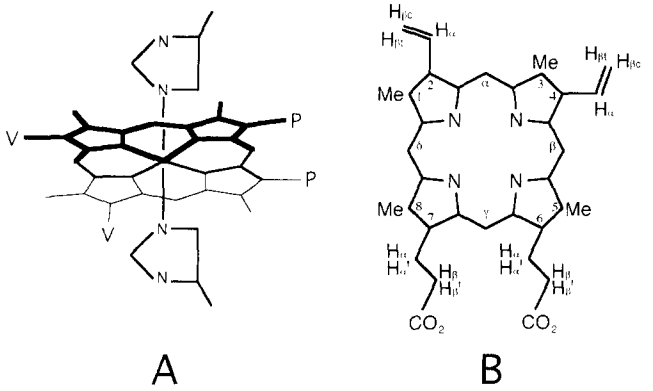

Fig. 1. The heme structure. A. The proposed bis-histidyl arrangement. *P* is propionate, and V is vinyl. B. Heme skeleton with the numbering system used in the text.

these systems by ^{1}H-NMR has increased through the use of multi-dimensional methods [24–26], yet no data have been reported for a paramagnetic molecule as large as heme · Hx. This report presents our initial data on heme · Hx, demonstrating that two-dimensional ^{1}H-NMR is practical and efficient in making resonance assignments. We demonstrate unambiguously that this complex is low-spin $S = 1/2$ paramagnetic, as it has two high-field axial histidine ligands. Using a variety of means, including specifically-deuterated hemes, we assigned several resonances in the hyperfine-shifted regions of the heme · Hx spectrum. In addition, a species comparison for heme · Hx is made, and evidence provided that the protein portion of this complex can exist in various folding states.

2. Materials and methods

2.1. Isolation of Hx

Hx from human and rat plasma was purified by affinity chromatography on heme-agarose [4,27]. Hx from cow and rabbit plasma was isolated by ion exchange and size-exclusion chromatography as described below for rabbit.

Hx was isolated from rabbit serum by a modification of the method of Noiva et al. [15]. 50 ml plasma were treated with an equal volume of saturated ammonium sulfate, stirred for 1 h at 25°C, and centrifuged at 12 000 × *g* for 1 h at 4°C. The supernatant was successively dialyzed against distilled water for 18 h, and 0.01 M sodium citrate at pH 5.9 for 18 h. The supernatant was concentrated (15 ml on a YM-30 Amicon ultrafiltration membrane), loaded onto a 'fast flow' CM-Sepharose 1.5 × 45 cm column, pre-equilibrated with 0.01 M sodium citrate, pH 5.9, and eluted with this buffer until emergence of the albumin containing fractions. An ion-exchange gradient (300 ml of 0.01 M to 300 ml of 0.1 M) of sodium citrate at pH 5.9 separated transferrin from co-eluting hemoglobin and Hx. Fractions were tested for heme binding ability by adding a small amount of heme to aliquots, recording absorption spectra in the visible region, and comparing them to standard heme · Hx spectra.

Heme was added to the combined heme binding fractions which were then incubated at 5°C for 1 h, and passed over a DEAE-Sephadex 1 × 8 cm column with 50 mM sodium phosphate, 100 mM NaCl, pH 7.3, to remove any excess heme. The heme-containing protein was concentrated on an Amicon YM-30 ultrafiltration membrane, and eluted at 14 ml h^{-1} from a Sephacryl S-200 column (95 × 2.5 cm) utilizing the same phosphate buffer. This gel exclusion step separated hemoglobin (the first band) from Hx (the second band), which was analysed for purity by SDS-PAGE (10% polyacrylamide) and with anti-transferrin anti-albumin antibodies on Western blots.

The fractions containing Hx · heme were pooled, exchanged into deuterated buffer (50 mM phosphate and 100 mM NaCl) at pH 7.5, and concentrated on an Amicon YM-30 ultrafiltration membrane to a volume of 200–500 μL for NMR experiments.

The deuterated hemes were donated by Professor Kevin Smith [28–30]. They were checked for fractional deuteration by recording the ^{1}H-NMR spectrum for each dicyano complex; each was seen to have < 10% residual proton resonance intensity for the labeled position.

2.2. NMR spectroscopy

NMR measurements were performed on a Bruker AMX-400 NMR spectrometer at 400.14 MHz, equipped with a dedicated 5 mm ^{1}H probe, at 40°C and pH 7.5 unless otherwise specified. Two-dimensional phase-sensitive NOESY [31] was used with TPPI [32]. 400 t_1 values were used, and free induction decays in t_2 were recorded in 1024 complex-point blocks, summing to 1024 acquisitions. The mixing time was 20 ms. Solvent suppression performed by saturation during the relaxation delay (30–200 ms) and the mixing time; the 90° transmitter pulse was ~ 8 μs. The data set was zero filled to 1024 × 1024 complex data point sets after digital filtering with a 30° phase-shifted sine-bell-squared function in both dimensions. Chemical shifts for all ^{1}H spectra were referenced to DSS through the residual water resonance at 4.51 ppm. Spectra were processed on the spectrometer X32 computer, using the manufacturer's software package, UXNMR.

Peak assignment strategies were as follows. First, deuterium isotope labels were used to assign specific heme methyls by their deletion in the reconstituted holoproteins. Second, the large chemical shifts and very broad linewidths were used to identify resonances from the axial ligands, now known to be histidines [17]. The two-dimensional NOESY spectroscopy is explained below.

3. Results

3.1. Species comparison

Spectra for heme · Hx from several species (heme complex of Hx_{human}, Hx_{cow}, Hx_{rat}, and Hx_{rabbit}) are shown in Fig. 2 A–D. The species dependency of the ^{1}H-NMR spectrum of heme · Hx is characteristic for each species. No other physical method previously used detects the species differences of Hx. The rabbit protein has by far the best signal-to-noise ratio. This finding is significant, and may reflect a relatively higher stability of the tertiary structure of Hx_{rabbit} than that of the other Hxs. We recorded the spectrum of Heme · Hx_{rabbit} over the pH range 6–9; no remarkable changes were seen in this range.

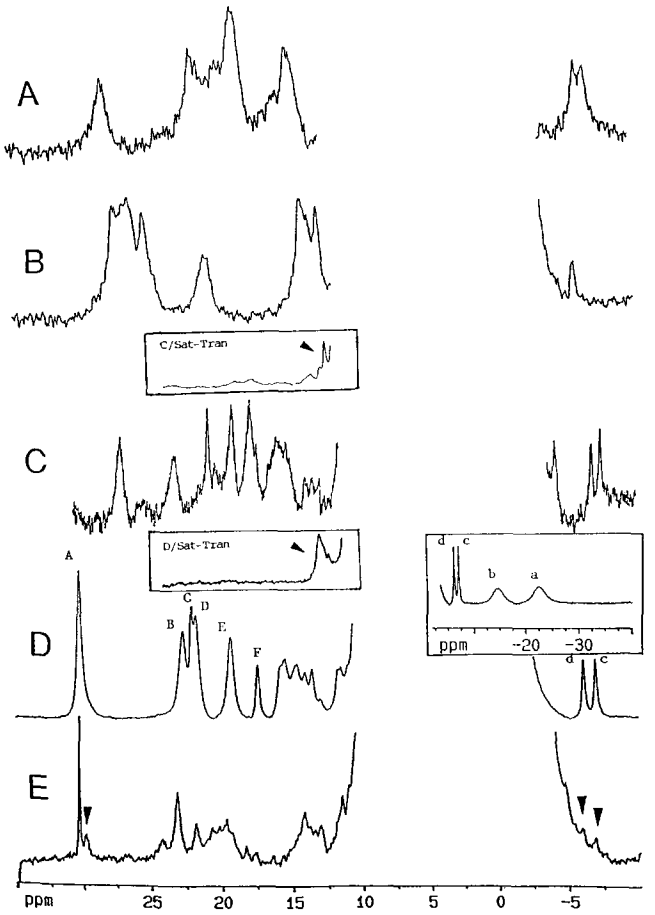

Fig. 2. Species comparison for the hyperfine-shifted portions of the ^{1}H-NMR spectrum of heme · Hx. A, Heme · Hx_{human}; B, heme · Hx_{cow}; C, heme · Hx_{rat}; D, heme · Hx_{rabbit}. The inset to trace C and the left inset to trace D show saturation-transfer difference spectra for the rat and rabbit proteins, recorded in 90% ^1H_2O/10% ^2H_2O solvent; thus the peaks in these spectra, indicated with arrows, are only from labile protons that are in fast exchange with the (saturated) bulk solvent. The right inset to trace D shows the more upfield region for heme · Hx_{rabbit}; this spectrum was recorded at very fast repitition rate to optimize detection of rapidly relaxing resonances. Note that the different species give rise to considerably different ^{1}H-NMR spectra, and that the rabbit spectrum is of much higher quality than from the other species. Assignments for lettered peaks are given in Table 1. E. heme · Hx_{rabbit}CN. The peaks marked with arrows may arise from heme · Hx_{rabbit}, although they do not have exactly the expected chemical shifts (see text).

Table 1
NMR parameters for heme · Hx_{rabbit} in ^2H_2O

Resonance [a]	Assignment	δ [b] (ppm)	δ_{dia} [c] (ppm)	T_1 [b] (msec)
A	$3CH_3$	30.12	−8	54
B	$8CH_3$	22.65	17	55
C	$2H_\alpha$	22.04	8	57
D		21.71	16	57
E	$1CH_3$	19.25	14	63
F		17.37	13	47
d	$2H_{\beta t}$	−6.16	12	59
c	$2H_{\beta c}$	−7.02	15	64
b	His-H_{ring} [d]	−14.5	13	≤ 2 [e]
a	His-H'_{ring} [d]	−22.6	19	≤ 2 [e]

[a] Peaks correspond to designations in Figs. 2, 3, and 4.
[b] Recorded at 40°C and pH 7.0.
[c] From extrapolations to $T^{-1} = 0$ (Curie plot).
[d] Tentative assignment.
[e] Estimated: T_1 too short for accurate determination under conditions used.

Although there are substantial spectral differences in A–D of Fig. 2, all of the spectra represent low-spin species, exhibiting similar hyperfine-shifted peaks, and likely have the same set of iron axial ligands. These ligands are presumably histidine residues, and our data confirms this in the following way. The inset to Fig. 2D shows that there are two broad resonances, at −22.6 (a) and at −14.5 (b) ppm. These peaks have short T_1 values (< 2 ms; Table 1) and are broad (short T_2 values), and so must be within a very short distance of the iron. Taking the distance for the heme Fe to methyl as 6.1 Å, the methyl $T_1 \approx 60$ ms (Table 1), and applying the equation for dipolar distance from the paramagnetic center (Fe) $T_1^i/T_1^j = (r_i/r_j)^6$, the protons giving peaks *a* and *b* must reside < 3.5 Å from the Fe. This distance resembles proximal His (F8) distance $r(C_{\delta,\varepsilon}H, Fe) \approx 3.4$ Å in myoglobin [33]. Further, there were no NOEs to the methyls (see below for these assignments) on irradiating peaks a and b in 1-dimensional experiments, confirming that these resonances are not due to heme *meso* protons. Our NMR data is therefore consistent with the proposed bis(histidyl) ligation of the heme iron in, at least, the rabbit protein.

The left insets to traces 2C and 2D are solvent-line saturation-transfer difference spectra for the rat and rabbit proteins, respectively, recorded in 90% ^1H_2O/10% ^2H_2O solvent using a binomial pulse sequence to suppress the solvent resonance. Spectra recorded by presaturation of the solvent resonance gave hyperfine-shifted regions indistinguishable from traces 2C and 2D. Thus, there are labile protons detected, likely from the two histidine ligands to the iron, but they are in sufficiently rapid exchange with the bulk solvent to preclude their observation if the solvent line is saturated.

Fig. 2E shows the result of adding cyanide to heme · Hx_{rabbit}. The only peaks visible in the paramagnetically resolved parts of the spectrum are within the chemical shift range and have linewidths that indicate that the cyanide adduct is low-spin. There are some small resonances (indicated by arrows) that are of similar chemical shift and pattern to the best resolved peaks in heme · Hx_{rabbit}. These peaks may be from a small fraction of the protein that was not converted to the cyanide adduct; however the chemical shifts are not identical to those in Fig. 2D. Until further work is performed we cannot distinguish whether these peaks arise from heme · Hx or from some other species, perhaps a heme-insertion isomer as found in other heme proteins ([34] for heme-insertion isomers in cytochrome b_5).

3.2. Peak assignments

Fig. 3 presents isotope-labeling experiments, performed by adding deuterated hemes to Hx_{rabbit}. These results demonstrate that the $1CH_3$, $8CH_3$, and $3CH_3$ resonances (see Fig. 1B for heme designations) are in the downfield spectral region, resolved from the envelope of protein resonances. No resonance is deleted from the hyperfine-shifted portions of the spectrum from the $5C^2H_3$-labeled material (Fig. 3B), so it appears that the $5CH_3$ lies within the −2 to 12 ppm region. This is the range of heme methyl chemical shifts observed for species that have substantial low-spin character [23]. The pattern of methyl chemical shifts is a consequence of the magnetic axes, and this, in turn, is largely governed by the orientations of the axial ligands [35], histidines in this case.

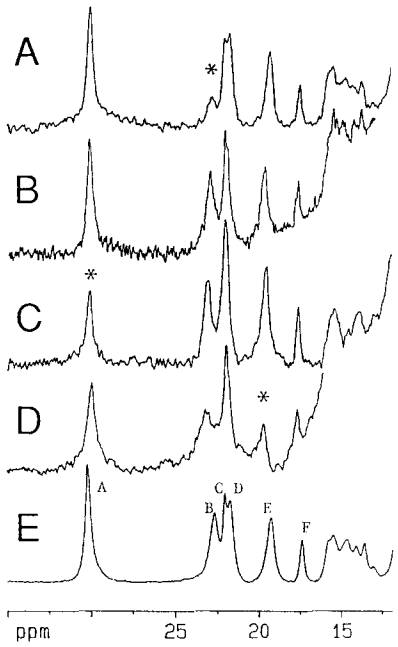

Fig. 3. ^{1}H-NMR spectra of heme·Hx_{rabbit} generated using isotopically-labeled hemin. A, $8C^2H_3$-heme·Hx_{rabbit}; B, $5C^2H_3$-heme·Hx_{rabbit}; C, $3C^2H_3$-heme·Hx_{rabbit}; D, $1C^2H_3$-heme·Hx_{rabbit}; E, heme·Hx_{rabbit}. Note that, although these spectra allow assignment of resonances, there is residual intensity for each peak. This might have resulted from some fraction of the Hx isolated from the serum being already complexed with heme, or from the presence of a heme-insertion isomer.

It is striking that none of the labeled resonances are entirely deleted, even though the hemes are deuterated to > 90% (see Section 2). It is possible that some of this

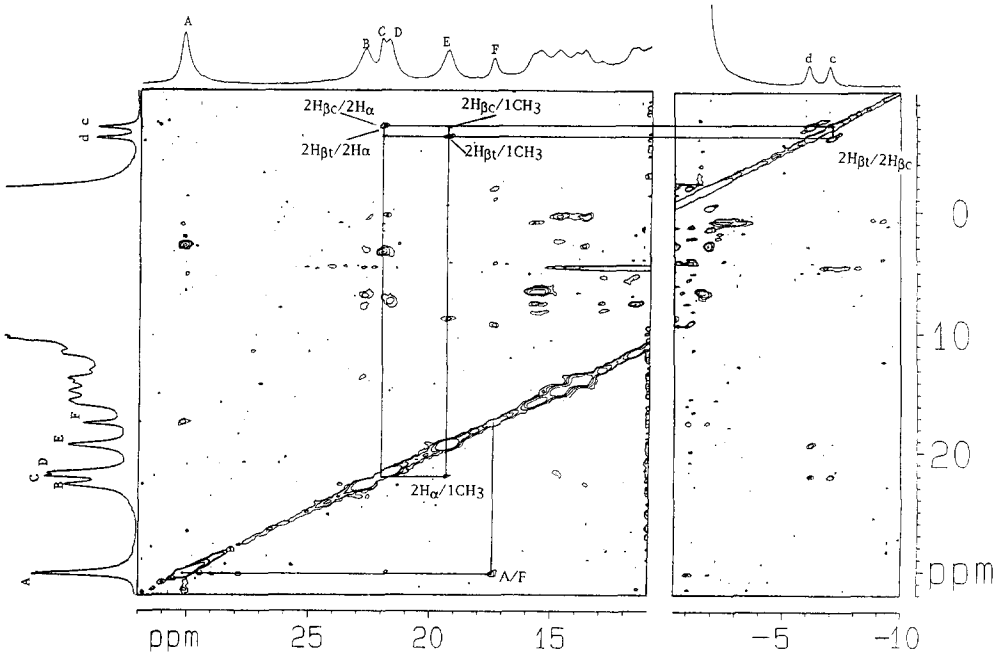

Fig. 4. Two-dimensional 20 ms mixing time NOESY and reference spectrum of heme · Hx_{rabbit}. Specific resonance assignments and correlations are indicated on the plot. Note that the NOEs are selective and of sufficient intensity to be useful for studying heme · Hx_{rabbit} in spite of the large size and carbohydrate content.

residual intensity arises from heme that was bound to protein before we isolated it from the serum. On the other hand, it is not likely that all of this residual intensity is from this source; it is more likely that some fraction of the complex exists as heme-insertion isomer(s) in heme · Hx; this would not be unusual for a noncovalent heme protein [34,44].

3.3. Two-dimensional ^{1}H-NMR spectroscopy: NOESY of heme · Hx_{rabbit}

Fig. 4 presents portions result of a two-dimensional NOESY spectrum of heme · Hx_{rabbit}. This species was chosen because of its relatively narrow resonance lines in the hyperfine-shifted portions of the spectrum. In this NOESY spectrum the $2H_\alpha$, $2H_{\beta c,t}$ spin system is evident from its NOEs to the adjacent $1CH_3$. These NOEs corroborate the assignment of the $1CH_3$ in the isotope labeling study (above). The $3CH_3$ (peak A) shows a strong NOE to a single proton resonance at 18.2 ppm (peak F), which may therefore be the vinyl $4H_\alpha$. This assignment is only tentative, however. The NOESY spectrum by itself is insufficient to allow unambiguous resonance assignments for the methyls nor for further heme periphery signals. Of the J-correlation spectra, MCOSY would be the most likely to be successful for a paramagnetic protein with large linewidths [24,26] We attempted this experiment, but no reliable cross-peaks were detected Therefore, we were forced to rely on only the isotope labeling and NOESY spectra. Table 1 summarizes the assignments, T_1 values, and temperature-dependencies of heme · Hx_{rabbit} hyperfine-shifted resonances.

4. Discussion

The hyperfine-shifted resonances of heme · Hx have properties which reflect that the complex is paramagnetic, low-spin. In particular, the linewidths, chemical shift range, and temperature-dependencies of these resonances allow this conclusion; previous electron paramagnetic resonance and circular dichroism [20,36,37] studies are in agreement. Thus, the *native complex* is 6-coordinate with strong-field ligands, consistent with histidine side chains-coordination at both the 5th and 6th Fe sites.

Further evidence for this model is found in the presence of the two very broad, upfield resonances in heme · Hx_{rabbit}. These resonances are extremely relaxed, so much so that one can assume that they arise from residues bound to the iron; only a coordinated residue in the immediate vicinity of the paramagnetic center would have such highly relaxed resonances in a low-spin complex. In low-spin axial histidine-ligated cases (examples: bis(imidazole)heme [38]; cytochrome b_5 [35–37]; myoglobin cyanide, and mutants [39–41]; cytochrome c peroxidase cyanide, and mutants [42]; horseradish peroxidase cyanide [43], the upfield paramagnetic shift of one histidine ring proton is generally accompanied by a similar downfield shift of the alternate ring proton. Therefore, the presence of two such upfield shifted resonances indicates the presence of two ligands, one at the 5th, and one at the 6th site. The alternate protons from the two ligated histidine rings are not apparent in the data presented here, but they may be located under the crowded regions of the spectra, either within the diamagnetic region or even in the 10 to 30 ppm region.

We had hoped to use the species-sensitivity of ^{1}H-NMR spectra to perform competition studies that would allow us to determine which Hx has the highest affinity for heme. Unfortunately, the rate of heme transfer is so slow that no heme transfer was observed even after several months, and so it is likely that the rate of heme release is significantly slower than the rate of denaturation of Hx.

The ligation pattern, with two histidines occupying both the 5th and 6th Fe sites, may help to explain the ability of Hx to inhibit heme-catalyzed oxidations. For these oxidations to be inhibited, oxygen may have its access to the heme blocked. This could happen either by the heme being buried in the protein matrix or by strong axial ligation. As mentioned in the Introduction, earlier studies have indicated that the heme is solvent exposed. The fact that the detected labile protons (Fig. 2) exchange quite rapidly supports this conclusion. Furthermore, at least when the iron is in the ferric state, the axial ligands are difficult to displace [22]. The data therefore suggests that the nature of the axial ligation leads to the antioxidant activity of Hx.

The most downfield peak in the heme · Hx_{rabbit}CN spectrum (Fig. 2E) is remarkably sharp. Some of the peaks of heme · Hx of the other species are also quite sharp (peak C [$2H_\alpha$] in Fig. 2D and the ~ 22 ppm peak in Fig. 2C for rabbit and rat proteins, for example). On the other hand, many heme · Hx resonances are very broad, especially in the cow and human proteins. We lowered the temperature for the highly-resolved rabbit protein in an attempt to detect evidence of conformational heterogeneity; however no *selective* broadening of resonances was observed. Another possible cause for the broadness of these resonances, and perhaps the extreme broadness in the peaks in the human (Fig. 2A) and cow (Fig. 2B) protein, is that the broadening is due to heterogeneity in the carbohydrate fraction of Hx. Covalent heterogeneity can lead to selective splitting and broadening of resonances in low-spin hemoproteins [34,44] analogous to what is seen here. An alternative explanation might be the presence of multiple folding patterns, perhaps between the two domains of the protein. Proteolytic digestion conditions have been reported [19,45] that will enable us to probe these possibilities; we are pursuing this line of investigation. Crystals have been obtained for the deglycosylated C-terminal domain [46]. That domain does not bind heme; however, if the two domains have similar three-dimensional structures [46,47], any structural information on the C-terminal do-

main of the protein may help shed light on the heme binding domain.

Acknowledgments

The specifically-deuterated porphyrins were a generous gift from Professor Kevin Smith (University of California at Davis). The authors are also indebted to Dr. Heli Nikkilä and Yi-Fang Chen for Hx isolations performed early in the work. This research was supported by a National Institutes of Health Grant DK-30203 and from the Robet Leet and Alara Guthrie Patterson Trust to U.M.-E., and the Medical Research Foundation of Oregon for a grant to D.H.P. Portland State University, the National Science Foundation, and the Murdock Charitable Trust are recognized for the purchase of the NMR spectrometer.

References

[1] Ursini, F., Maiorino, M., Ferri, L., Valente, M. and Gregolin, C. (1981) J. Inorg. Biochem. 15, 163–169.
[2] Aft, R.L. and Mueller, G.C. (1985) Life Sci. 36, 2153–2161.
[3] Aft, R.L. and Mueller, G.C. (1984) J. Biol. Chem. 259, 301–305.
[4] Muller-Eberhard, U. (1988) Methods Enzymol. 163, 536–565.
[5] Vincent, S.H., Grady, R.W., Shaklai, N., Snider, J.M. and Muller-Eberhard, U. (1988) Arch. Biochem. Biophys. 265, 539–550.
[6] Gutteridge, J.M.C. and Smith, A. (1988) Biochem. J. 256, 861–865.
[7] Hrkal, Z., Vodrázka, Z. and Kalousek, I. (1974) Eur. J. Biochem. 43, 73–78.
[8] Smith, A. and Morgan, W.T. (1979) Biochem. J. 182, 47–54.
[9] Potter, D., Chroneos, Z.C., Baynes, J.W., Sinclair, P.R., Gorman, N., Liem, H.H., Muller-Eberhard, U. and Thorpe, S.R. (1993) Arch. Biochem. Biophys. 300, 98–104.
[10] Nikkilä, H., Gitlin, J.D. and Muller-Eberhard, U. (1991) Biochemistry 30, 823–829.
[11] Muller-Eberhard, U., Liem, H.H., Hanstein, A., Saarinen, P.A. (1969) J. Lab. Clin. Med. 73, 210–218.
[12] Foidarte, M., Eiseman, J., Engel, W.K., Adornato, B.T., Liem, H.H. and Muller-Eberhard, U. (1982) J. lab. Clin. Med. 100, 451–460.
[13] Solar, I., Muller-Eberhard, U. and Shaklai, N. (1989) FEBS Lett. 256, 225–229.
[14] Goldfarb, V., Trimble, R.B., De Falco, M., Liem, H.H., Metcalfe, S.A., Wellner, D. and Muller-Eberhard, U. (1986) Biochemistry 25, 6555–6562.
[15] Noiva, R., Pete, M.J. and Babin, D.R. (1987) Comp. Biochem. Physiol. 88B, 341–347.
[16] Morgan, W.T., Sutor, R.P. and Muller-Eberhard, U. (1976) Biochim. Biophys. Acta 434, 311–323.
[17] Morgan, W.T., Muster, P., Tatum, F., Kao, S., Alam, J. and Smith, A. (1993) J. Biol. Chem. 268, 6256–6262.
[18] Morgan, W.T. and Muller-Eberhard, U. (1976) Arch. Biochem. Biophys. 176, 431–441.
[19] Muster, P., Tatum, F., Smith, A. and Morgan, W.T. (1991) J. Protein Chem. 10, 123–128.
[20] Morgan, W.T. and Vickery, L.E. (1978) J. Biol. Chem. 253, 2940–2945.
[21] Muller-Eberhard, U. and Grizzuti, K. (1971) Biochemistry 10, 2062–2066.
[22] Hrkal, Z., Kalousek, I. and Vodrázka, Z. (1981) Studia Biophysica, 82, 69-73.
[23] Satterlee, J.D. (1986) Annu. Rep. NMR Spectrosc. 17, 79–178.
[24] Peyton, D.H. (1991) Biochem. Biophys. Res. Commun. 175, 515–519.
[25] Satterlee, J.D. and Erman, J.E. (1991) Biochemistry 30, 4398–4405.
[26] Yu, L.P., La Mar, G.N. and Rajarathnam, K. (1990) J. Am. Chem. Soc. 112, 9527–9534.
[27] Tsutsui, K and Mueller, G.C. (1982) Anal. Biochem. 121, 244–250.
[28] Smith, K.M., Leung, H.-K. and Parish, D.W. (1986) J. Chem. Res. (S) 324–325.
[29] Smith, K.M., Leung, H.-K. and Parish, D.W. (1986) J. Chem. Res. (M) 2743–2761.
[30] Smith, K.M., Miura, M. and Morris, I.K. (1986) J. Org. Chem. 51, 4660–4667.
[31] Kumar, A., Ernst, R.R. and Wüthrich, K. (1980) Biochem. Biophys. Res. Commun. 95, 1–6.
[32] Marion, D. and Wüthrich, K. (1983) Biochem. Biophys. Res. Commun. 113, 967–974.
[33] Takano, T. (1977) J. Mol. Biol. 110, 537–568.
[34] La Mar, G.N., Burns, P.D., Jackson, J.T., Smith, K.M., Langry, K.C. and Strittmatter, P. (1981) J. Biol. Chem. 256, 6075–6079.
[35] McLachlan, S.J., La Mar, G.N. and Lee, K.-B. (1988) Biochim. Biophys. Acta 957, 430–445.
[36] Aisen, P., Leibman, A. and Harris, D.C. (1974) J. Biol. Chem. 249, 6824–6827.
[37] Bearden, A., Morgan, W.T. and Muller-Eberhard, U. (1974) Biochem. Biophys. Res. Commun. 61, 265–272.
[38] Chacko, V.P. and La Mar, G.N. (1982) J. Am. Chem. Soc. 104, 7002–7007.
[39] Emerson, S.D. and La Mar, G.N. (1990) Biochemistry 29, 1545–1556.
[40] Emerson, S.D. and La Mar, G.N. (1990) Biochemistry 29, 1556–1566.
[41] Rajarathnam, K., La Mar, G.N., Chiu, M.L. and Sligar, S.G. (1992) J. Am. Chem. Soc. 114, 9048–9058.
[42] Satterlee, J.D., Erman, J.E., Mauro, J.M. and Kraut, J. (1990) Biochemistry 29, 8797–8804.
[43] Thanabal, V., de Ropp, J.S. and La Mar, G.N. (1987) J. Am. Chem. Soc. 109, 7516–7525.
[44] Peyton, D.H., Krishnamoorthi, R., La Mar, G.N., Gersonde, K., Smith, K.M. and Parish, D.W. (1987) Eur. J. Biochem. 168, 377–383.
[45] Morgan, W.T. and Smith, A. (1984) J. Biol. Chem. 259, 12001–12006.
[46] Baker, H.M., Norris, G.E., Morgan, W.T., Smith, A. and Baker, E.N. (1993) J. Mol. Biol. 229, 251–252.
[47] Takahashi, N., Takahashi, Y. and Putnam, F.W. (1985) Proc. Nat. Acad. Sci., U.S.A. 82, 73–77.